Central regulation of the pharyngeal and upper esophageal reflexes during swallowing in the Japanese eel.

Takao Mukuda* and Masaaki Ando[1]

Laboratory of Integrative Physiology, Graduate School of Integrated Arts and Sciences, Hiroshima University, 1-7-1 Kagamiyama, Higashi-hiroshima 739-8521, Japan

[1]Present address: Laboratory of Physiology, Ocean Research Institute, The University of Tokyo, 1-15-1 Minamidai, Tokyo 194-8639, Japan

Page Count: 31 pages (including references and figure legends)

Tables and Figures: 0 tables, 7 figures

Supplement figures: 2 figure

*Corresponding author:

Takao Mukuda, Laboratory of Integrative Physiology, Graduate School of Integrated Arts and Sciences, Hiroshima University. 1-7-1 Kagamiyama, Higashi-hiroshima 739-8521, Japan.

Email: mtakao@hiroshima-u.ac.jp

Phone: +81-82-424-6403

Fax: +81-82-424-0759

Abstract

We investigated the regulation of the pharyngeal and upper esophageal reflexes during swallowing in eel. By retrograde tracing from the muscles, the motoneurons of the upper esophageal sphincter (UES) were located caudally within the mid region of the glossopharyngeal-vagal motor complex (mGVC). In contrast, the motoneurons innervating the pharyngeal wall were localized medially within mGVC. Sensory pharyngeal fibers in the vagal nerve terminated in the caudal region of the viscerosensory column (cVSC). Using the isolated brain, we recorded 51 spontaneously active neurons within mGVC. These neurons could be divided into rhythmically (n=8) and continuously (n=43) firing units. The rhythmically firing neurons seemed to be restricted medially whereas the continuously firing neurons were found caudally within mGVC. The rhythmically firing neurons were activated by the stimulation of the cVSC. In contrast, the stimulation of the cVSC inhibited firing of most but not all the continuously firing neurons. The inhibitory effect was blocked by prazosin in 17 out of 38 neurons. Yohimbine also blocked the cVSC-induced inhibition in 5 of prazosin-sensitive neurons. We suggest that the neurons in cVSC inhibit the continuously firing motoneurons to relax the UES and stimulate the rhythmically firing neurons to constrict the pharynx simultaneously.

Keywords: Swallowing, Esophagus, Medulla oblongata, Vagal nerve, Catecholamines, Japanese eel

Abbreviations

aCSF, artificial cerebrospinal fluid; AP, area postrema; BBB, blood-brain barrier; BDA-10KF, biotinylated dextran amine conjugated with fluorescein isothiocyanate; ChAT, choline acetyltransferase; CNC, commissural nucleus of the Cajal; cVSC, caudal region of VSC; EB, Evans blue; GVC, glossopharyngeal-vagal motor complex; mGVC, mid region of GVC; PBS, phosphate buffered saline; TH, tyrosine hydroxylase; UES, upper esophageal sphincter; VSC, viscerosensory column

Introduction

Swallowing is an essential behavior associated with drinking or ingestion in all vertebrates, including fish. This behavior requires the precisely coordinated control of muscles in the oropharyngeal region. Muscular action is coordinated by both the central and peripheral nervous systems. The central components involved in swallowing are well known in vertebrates including fish, and their morphological organization has been reported in a number of teleost species such as goldfish (Morita and Finger 1987; Goehler and Finger 1992) and catfish (Kanwal and Caprio 1987). The central swallowing reflex circuits are localized in the caudal medulla. Central sensation from the oropharyngeal region is detected by the dorsal viscerosensory neurons. Conversely, motor innervation of the muscles involved in swallowing originates in the ventromedial visceromotor neurons of the glossopharyngeal and the vagal nerves. Although the direct afferent connections to the visceromotor nuclei are still unclear, anterograde tracing has revealed some projections to the visceromotor nuclei from the viscerosensory neurons (Morita and Finger 1985; Goehler and Finger 1992).

In the Japanese eel, morphological and functional features of the vagal motor components are relatively well understood but little is known about the sensory reception. Motoneurons of swallowing-associated muscles, such as the pharyngeal wall and upper esophageal sphincter (UES), are viscerotopically arranged in the glossopharyngeal-vagal motor complex (GVC). These motoneurons are cholinergic (Mukuda and Ando 2003a) and constrict the pharyngeal muscle and UES through acetylcholine (Kozaka and Ando 2003). Ito et al. (2006) in the eel reported that motor neurons in GVC fire spontaneously at high frequency using the isolated brain specimens

and the firing activity was inhibited by catecholamines.

The viscerosensory neurons form a long viscerosensory column (VSC) in the dorsal medulla in the eel and the VSC lacks specialized, hypertrophied glossopharyngeal and vagal lobes (Mukuda and Ando 2003b) as in the gray mullet (Díaz-Regueira and Anadón 1992) and the rainbow trout (Folgueira et al. 2003) although it is well known to possess the highly specialized, protruded vagal lobe in the goldfish (Morita and Finger 1987; Goehler and Finger 1992) and the catfish (Kanwal and Caprio 1987). Thus, it has been difficult to differentiate individual nuclei strictly in the eel. In general, however, there has been little effort to systematically study the neurophysiologic features of these swallowing-related nuclei, and their connections, in teleosts.

The entrance of esophagus is normally held closed by tonic contraction of the UES. This facilitates breathing in both fish and mammals. The process of swallowing requires coordination of the upper esophageal relaxation and pharyngeal contractile reflexes to transport pharyngeal contents into the esophagus. The reflexes are triggered by pharyngeal stimulation, that is, attachment of pharyngeal contents, such as food and water, to the pharyngeal wall (Medda et al. 1994). Thus, the central system controlling the UES relaxation following the sensation of inputs from the pharynx is an important component to coordinate swallowing reflex. However, despite their importance little is known about the central regulation of these reflexes.

To reveal the central systems controlling the pharyngeal contraction and upper esophageal relaxation reflexes in the Japanese eel, we identified the motoneurons innervating the UES and pharyngeal wall in the mid region of GVC (mGVC), and searched candidates of neuronal pathways and neurotransmitters regulating the mGVC

neurons. To better localize the motoneurons of the UES and pharyngeal wall within mGVC than previously reported (Mukuda and Ando 2003a), we injected a retrograde fluorescent dye, Evans blue (EB), into the concerned muscles, using an improved method. In addition we also injected biotinylated dextran amine conjugated with fluorescein isothiocyanate (BDA-10KF) into the vagal nerve bundle distributed in the pharyngeal wall and branchial arches to determine the reception sites for sensory inputs in the caudal medulla. We then recorded neuronal activity in mGVC in response to electric field stimulation of the caudal region of VSC (cVSC). Last, we investigated the involvement of catecholamines during the control of motoneuron activity using the receptor antagonists, prazosin and yohimbine.

Materials and methods

Cultured Japanese eels, *Anguilla japonica* (n = 49, ~200 g) were obtained from a commercial source. The eels were held in artificial seawater aquaria (20°C), without food, for at least one week before use.

To study the distribution of the motoneurons innervating the pharyngeal wall and UES, we injected a retrograde fluorescent tracer, EB (green excitation, red emission, 1422-52, Kanto Chemical, Tokyo, Japan), into the pharyngeal wall (n = 5) or UES (n = 44). Out of 44 eels injected with EB into the UES, 7 eels were employed for immunohistochemistry, 6 were for BDA-10KF staining and the rest 31 were for electrophysiology. The eel was anesthetized by immersion in 0.1% tricaine methanesulfonate (A5040, Sigma, St Louis, MO) dissolved in artificial seawater

buffered with 0.3 % $NaHCO_3$. To open a mouth wide and expose the UES, a mouthpiece made by a conical sampling tube (ST-500, BIO-BIK) which the tip was cut (diameter of the cutting end: 5 mm) was inserted into the oral cavity, 20 µl EB solution (5.0 mg/ml, dissolved in phosphate buffered saline, PBS, pH 7.4) was injected into the left UES by a syringe with a thin needle (33 gages). To inject EB into the pharyngeal wall, the mouthpiece was not necessary. After injection, the animal was returned to the aquarium and kept for at least 3 days. Some of the eels injected with EB into the UES were also injected with a neuronal tracer, BDA-10KF (SP-1130, Vector, Burlingame, CA), into the pharyngeal fibers of vagal nerve (n = 6), which projects to the pharyngeal wall and branchial arches caudal to the 3rd branchial arch but not to the UES. Following the injection of EB, the epidermal layer of the branchial chamber covered by the operculum was removed to expose a vagal nerve trunk under the anesthesia. Under a stereoscopic microscope (MS 5, Leica, Wetzlar, Germany), 20 µl BDA-10KF solution (5.0 mg/ml in PBS) was injected into the vagal nerve via a glass capillary by air pressure. After injections, the eels were sutured, and returned to the aquaria to recover for one week.

Following the recovery period, the eel was anaesthetized and perfused transcardially with PBS and followed by 4% paraformaldehyde in 0.1 M phosphate buffer (pH 7.4). The skull was then fenestrated and immersed in the fixative overnight at 4°C. After the fixation, the brain was isolated from the skull, and cryoprotected with 30% sucrose in 0.1 M phosphate buffer and embedded. The transverse or horizontal sections (14 µm thick) were made using a frozen microtome (CM1850, Leica) and mounted on MAS-coated glass slides (S9441, Matsunami Glass, Osaka, Japan). To examine the staining by EB, the mounted sections were immediately photographed

under a fluorescent microscope (Eclipse E600, Nikon, Tokyo) equipped with a digital camera (DXM1200F, Nikon). Following this, the sections were frozen at -80°C until further use.

The catecholaminergic neurons as well as the cholinergic neurons were visualized by immunohistochemistry. All the operations without notation of the condition were carried out at room temperature. After rinsing three times in PBS, the sections were treated with a blocking solution containing 5% normal donkey serum, 0.1% Triton X-100 and 0.05% Tween 20 in PBS for 1 h. A rabbit polyclonal antibody raised against tyrosine hydroxylase (TH) from rat phenochromocytoma (1: 500, AB152, Chemicon, Temecula, CA) and a goat polyclonal antibody raised against choline acetyltransferase (ChAT) from human placental (1: 500, AB144, Chemicon) were applied for 24-48 h at 4°C. After rinsing three times in PBS, the sections were treated with the secondary antibodies, Cy2-conjugated donkey anti-rabbit IgG (1: 500, 711-225-152, Jackson, West Grove, PA) and Cy3-conjugated donkey anti-goat IgG (1: 500, 705-165-147, Jackson), together with 4',6-diamidino-2-phenylindoledihydrochloride (1:1000, D9564, Sigma) to counterstain, were applied for 2 h. After rinsing three times in PBS, the sections were coverslipped. The sections were examined and photographed under a fluorescent microscope (BZ-9000, Keyence, Osaka, Japan). Primary antibodies employed in the present study are widely used for immunohistochemistry in fish: anti-TH antibody (e.g. Sueiro et al. 2003 in dogfish; Barreiro-Iglesias et al. 2008 in lamprey; Mukuda et al. 2005 in Japanese eel; Castro et al. 2008 in trout; Ma 1994 in zebrafish); anti-ChAT antibody (e.g. Anadón et al. 2000 in dogfish; Pombal et al. 2001, 2003 in lamprey; Clemente et al. 2004; Arenzana et al. 2005 in zebrafish), and we did not observe any immunoreactivity

in the absence of the primary antibodies.

To intensify the staining of BDA-10KF, we developed every other section of the caudal medulla with ABC kit (PK-6100, Vector). The sections were pretreated with PBS containing 0.3% Triton X-100 and 0.05% Tween 20 for 10 min. The sections were immersed in 5% H_2O_2 in methanol for 30 min, rinsed three times with PBS, and then incubated with the avidin-biotin complex (1: 100) overnight at 4°C. After rinsing, the sections were incubated with 0.05% 3,3'-diaminobenzidine tetrahydrochloride (Nakarai Tesque, Tokyo, Japan) in phosphate buffer for 30 min to intensify colorization. The sections were then treated with 0.05% 3,3'-diaminobenzidine tetrahydrochloride in phosphate buffer containing 0.01% H_2O_2 and 0.04% $NiCl_2$ for 5 min in dark. Finally, the sections were rinsed, dehydrated, cleared and coverslipped. The sections were examined with a light microscope (Eclipse E600, Nikon). The remaining sections were stained with anti-TH antibody and examined under the fluorescent microscope (BZ-9000, Keyence) according to the immunohistochemical procedures as described before.

To prepare the specimen for electrophysiology, we decapitated the eel injected with EB into the UES (n = 31). The muscular tissue around the skull was removed and the cranium was placed in artificial cerebrospinal fluid (aCSF: 124 mM NaCl, 5 mM KCl, 1.3 mM $MgSO_4$, 1.2 mM $CaCl_2$, 1.2 mM $NaHPO_4$, 26 mM $NaHCO_3$, 10 mM glucose) during the operations. All the bones, with the exception of the palatal bone, were removed to expose the brain. The whole brain (between the olfactory bulb and the rostralmost spinal cord), associated with the palatal bone, was tied to an acryl plate and set in the experimental chamber (~2 ml volume). The chamber was continuously perfused with aCSF (1.0 ml/min) and maintained at 20°C. A gas mixture of 95% O_2 and

5% CO_2 (pH 7.4) was bubbled into the aCSF in the reservoir.

To record neuronal activity, we used a tungsten electrode (5 μm tip diameter; KU207-010, Unique Medical, Tokyo, Japan). The electrode was slowly inserted into mGVC to record extracellular spiking activity. An Ag-AgCl reference electrode was placed in aCSF in the chamber. The neuronal activity of the mGVC neurons was filtered at 15-3k Hz and then amplified. The signals were digitized by an AD converter (Power Lab 2/25, ADInstruments, Bella Vista, Australia) at a sampling rate of 40k Hz. We recorded the electrical activity of mGVC in an area ranging from 0 to 280 μm rostral to the obex. This area is dominated by motoneurons that innervate the UES (Mukuda and Ando 2003a). These neurons typically fire spontaneously and show large amplitude spikes (>75 μV) (Ito et al. 2006).

To apply electric field stimulation we used a bipolar electrode manufactured by combining the two tungsten electrodes mentioned above. The distance between the tips of two electrodes was 10-30 μm. The stimulating electrode was placed on the dorsal surface of the medulla at the level of the obex and immediately above the cVSC, which is ipsilateral to the recording site. As a stimulus, three electrical pulses (0.5 mA, 0.1 msec) were applied at 10 Hz.

We examined the effects of two antagonists for catecholamine receptors (prazosin and yohimbine) on the action of cVSC stimulation. Drugs (1 μM final concentration) were added to the aCSF bath via a series of manually operated valves. Prazosin was used as a nonspecific catecholamine receptor antagonist in the eels, and yohimbine as a specific adrenoceptor antagonist (Ito et al. 2006).

After the electrophysiological recordings, the recording site was checked histologically (Supplement figure 2). Each brain was fixed in 4% paraformaldehyde in

0.1 M phosphate buffer (pH 7.4) overnight at 4°C, cryosectioned, and immunostained as described before.

Offline analyses of the digitized signals were made by Chart Pro (ADInstruments). The single-units were separated based on the distribution pattern of the amplitude and width of spikes during a 300 sec period. Spikes with an amplitude <75 μV were omitted. To evaluate the effect of field stimulation of cVSC on mGVC, the mean spike counts during a 5 sec period at 30 sec before the stimulation, immediately after the stimulation, and 30 sec after the stimulation were compared. The trial was replicated five times in each experiment. Comparison of the mean spike count during each time epoch was performed by Tukey-Kramer *post hoc* test. The differences were considered significant at $P < 0.01$.

Results

Motoneurons innervating the pharyngeal wall and upper esophageal sphincter

Following the injection of EB into the pharyngeal wall or UES, the neurons in mGVC which was ipsilateral to the injection site were stained (Fig. 1a-d). As shown in a summary diagram of the rostrocaudal distribution of motoneurons stained with EB, the neurons innervating the pharyngeal wall were distributed in the mid region of mGVC (Fig. 1f). In contrast, the neurons innervating the UES were distributed in more caudal region within mGVC (Fig. 1f). In the region between 238-280 μm rostral to the obex, both motoneurons were co-existed (Fig. 1f). In the case of eels injected with

BDA-10KF into the pharyngeal branch of vagal nerve, similarly, the BDA-10KF-positive motoneurons were located more rostral to EB-positive neurons within mGVC (data not shown). All the EB-positive neurons were ChAT-immunoreactive (Fig. 1a, b), indicating that they are cholinergic.

TH-immunoreactive fibers were found abundantly around the neurons innervating the UES (Fig. 1b-d) and to a lesser extent around the neurons innervating the pharyngeal wall (Fig. 1a). A summary of the rostrocaudal distribution of TH-immunoreactive neurons is shown in Fig. 1f. Although TH-immunoreactive fibers were relatively widespread throughout the medulla, the strongest signal was observed around the mGVC neurons innervating the UES and the dorsal region along the wall of the fourth ventricle (Fig. 1c, d). The cell bodies of these TH-immunoreactive fibers were localized in the cVSC (Fig. 1e). The TH-immunoreactive cell bodies in cVSC were observed in the dorsal medulla from the paired region (Supplement figure 1c-f) to the obecular region (Supplement figure 1g-i) in cVSC. Neurons of the area postrema (AP) were also TH-immunoreactive in the postobecular region, but their cell bodies were located outside the blood-brain barrier (BBB) (Supplement figure 1j-p) and their fibers were entered into the caudal region of GVC, not into mGVC.

Sensory inputs into the dorsal medulla from the pharyngeal region

BDA-10KF-positive nerve fibers were traced to the ipsilateral, but not contralateral, caudal region of the dorsal medulla. The BDA-10KF-positive fibers were divided into two types: (1) those showing thin fibers alone (Fig. 2a, b) and (2) those forming tubercles at the end of the thin fibers in cVSC (Fig. 2a, d). The tubercles were

tadpole-shaped (Fig. 2d) and 4-8 μm in width. There were BDA-10KF-positive cell bodies in the nodose ganglion (Fig. 2c), and their fibers entered the medulla via the vagal nerve, coursed along the dorsolateral margin of the DV, and terminated in the cVSC (Fig. 2b, d). Fig. 2e illustrates the TH-immunostaining of the section immediately rostral to the one shown in Fig. 2d. The cVSC contained a large number of TH-immunoreactive neurons (Fig. 2e). The section shown in Fig. 2b is almost same sectioning level of that in Fig. 2e. In the paired region of VSC, TH-immunoreactive neurons were predominant more caudally (Supplement figure 1d-f), compared rostrally (Supplement figure 1a-c). These suggest that the sensory inputs from the pharyngeal region are transmitted into the catecholaminergic neurons in cVSC exclusively.

Effect of viscerosensory activation on spontaneous activities of the mid region of glossopharyngeal-vagal motor complex

We recorded spontaneous neuronal activities in the mGVC neurons and examined the effects of the stimulation of cVSC in the eels which were injected EB into the UES at least 3 days before the electrophysiological recording. The recording positions are summarized in Fig. 3. The majority of the recordings were made within the caudal region of mGVC, which contains the neurons innervating the UES. We also made two recordings in the mid region of mGVC. In this region, the motoneurons innervating the UES or the pharynx were co-located (Figs. 1f, 3).

We obtained 31 multi-unit extracellular recordings from mGVC. The neurons could be divided into two categories based on the spontaneous firing patterns. The one category includes neurons that show rhythmical activities of an interval of several

seconds (Fig. 4a). The other includes the neurons that fire continuously (Fig. 4b). To obtain single-unit activity, we tried to classify the units in 31 extracellular recordings as described in Materials and methods and discriminated 51 single-units (Fig. 4c).

Eight single-units displayed a “rhythmic firing” activity and were found in the mid region of mGVC (+224-+280 from the obex). When the electric field stimulation of cVSC was applied during the interval of the spontaneous bursting interval, these neurons were activated immediately (Fig. 5a). As a result, the next burst was significantly delayed. However, spontaneous firing pattern was resumed rather quickly and the burst interval was restored to pre-stimulation levels. To investigate the involvement of the catecholamines in the excitatory effect by the cVSC stimulation, similar experiments were repeated in the presence of prazosin, a non selective catecholamine receptor antagonist in eels or yohimbine, a selective adrenoceptor antagonist (Ito et al. 2006). The excitatory action of the cVSC stimulation on the rhythmically bursting neurons was not affected by these catecholamine receptor antagonists (data not shown).

Forty-three single-units displayed a “continuous firing” activity. The neurons showing this type of activity were recorded throughout the caudal region of the mGVC. Fig. 5b illustrates the effect of the cVSC stimulation on mGVC activity. Spontaneous firing activity was transiently inhibited immediately after the stimulation of cVSC (Fig. 5b). The single-unit analysis of the recorded activities is presented in Fig. 5c. The number of spikes was decreased in all the detected units (a-d) immediately after the stimulation (Fig. 5c). This inhibitory effect was suppressed in the unit a, b, or d, but not in c by prazosin (Fig. 5c). Yohimbine suppressed the inhibitory effect in the unit a and b, but not in the unit c and d (Fig. 5c). The effect of prazosin and yohimbine were

completely reversed by washing out of the drugs (Fig. 5c).

The inhibitory effect of cVSC stimulation on mGVC is summarized in Fig. 6. Forty three units were from the continuously firing neurons. Of these, 38 were inhibited by the cVSC stimulation and none of them were activated by the cVSC stimulation (Fig. 6). We observed no effect in five units (Fig. 6). Seventeen of the cVSC stimulation-responsive units were sensitive to prazosin (Fig. 6). Of these, five units were also sensitive to yohimbine while the remainders were insensitive (Fig. 6).

Discussion

Control in neuronal activities of the glossopharyngeal-vagal motor complex

This is the first report to show that the teleost mGVC is controlled by inputs from cVSC. Our results suggest that cVSC exerts both excitatory and inhibitory control of the mGVC neurons. The inhibition induced by the cVSC stimulation is found in most of the mGVC neurons which fire continuously (38 out of 43 neurons). The inhibitory effect was suppressed by prazosin in 17 out of 38 neurons. In addition, the cVSC-induced inhibition was also suppressed with yohimbine in 5 out of 17 prazosin-sensitive neurons. Prazosin is a non-selective catecholamine receptor antagonist whereas yohimbine is a selective adrenoceptor antagonist in the Japanese eel (Ito et al. 2006). Therefore, noradrenaline/adrenaline is involved in 5 neurons sensitive to both prazosin and yohimbine (13% in neurons inhibited by the cVSC stimulation), and dopamine is likely to be involved in the remaining 12 neurons that are inhibited by prazosin but not by

yohimbine (32%). The excitation by the cVSC stimulation is observed in all the rhythmically firing neurons. Since prazosin as well as yohimbine had no effect on the activation of rhythmically firing neurons, these neurons seem to receive non-catecholaminergic excitatory inputs from cVSC.

We have shown previously that microapplication of dopamine or noradrenaline/adrenaline to the mGVC induces inhibition of the continuously firing neurons in the eel (Ito et al. 2006). In the present study, we observed that the fibers of TH-immunoreactive neurons within cVSC project to the mGVC along the wall of fourth ventricle and the TH-immunoreactivity overlaps with the mGVC motoneurons stained by EB from the UES. The synaptically evoked-inhibition of mGVC by the cVSC stimulation was suppressed by catecholamine receptor antagonists. These suggest a possibility that the catecholaminergic neurons in cVSC inhibit directly the mGVC motoneurons which innervate the UES. In mammals direct synaptic contacts have been demonstrated between the viscerosensory neurons in the nucleus of the solitary tract which receive the vagal afferents from the pharyngeal apparatus (Hudson, 1986) and the vagal motoneurons in the nucleus ambiguus which innervate the UES (Hayakawa et al. 1997). Electrophysiological studies have shown that the neurons in nucleus of the solitary tract project directly to dorsal motor nucleus of the vagal nerve which contains motoneurons of the stomach and intestine. Around 10% of the neurons in dorsal motor nucleus of the vagal nerve are inhibited by the stimulation of nucleus of the solitary tract via the action of noradrenergic α2-receptors (Fukuda et al. 1987). Inhibitory effect of the nucleus of the solitary tract activation on dorsal motor nucleus of the vagal nerve is, however, primarily mediated by GABA (Feng et al. 1990; Travagli et al. 1991; Washabau et al. 1995; Broussard et al. 1997; Sivarao et al. 1998). Excitation of the

neurons in dorsal motor nucleus of the vagal nerve by the stimulation of nucleus of the solitary tract is mediated primarily by glutamate (Willis et al. 1996; Broussard et al. 1997; Sivarao et al. 1999; Laccasagne and Kessler 2000; Nabekura et al. 2002). Further experiments are required to determine whether the connections between cVSC and mGVC are monosynaptic or not in the Japanese eel.

Topography of the viscerosensory and visceromotor nuclei

We were able to determine that mGVC is controlled by cVSC, not by AP, since we stimulated cVSC precisely in the present study. In addition, in a preliminary experiment, we observed that the stimulation of AP was no effect on the spontaneous activity of mGVC (data not shown). AP and cVSC are close each other and these nuclei contain TH-immunoreactive neurons. However, we distinguished AP clearly since AP shows a grooved, reddish midline structure due to well-developed vascularization in the postobecular region on the dorsal aspect in the Japanese eel (Mukuda et al. 2005). Histologically, AP is located outside the BBB in the postobecular region (Supplement figure 1j-p) whereas cVSC is inside the BBB in the paired and obecular region (Supplement figure 1 a-i). Roberts et al. (1989) in the European eel has described that dopamine neurons are distributed rostracaudally in the dorsal medulla ranging from the paired and postobecular regions immunohistochemically and that this dopaminergic group is referred to AP. But, this assignment seems to contain both AP and cVSC components since the postobecular region lacks the BBB.

In the eel VSC, the vagal lobe and commissural nucleus of the Cajal (CNC) are not discriminated strictly yet and the histological assignment is confused since the eel

VSC forms a rostrocaudal long column containing the components of vagal lobe and CNC as in the gray mullet (Díaz-Regueira and Anadón 1992) and the rainbow trout (Folgueira et al. 2003). Roberts et al. (1989) has found vagal lobe in the rostral region of VSC at which the cerebellar crest emerges in the European eel, while Ito et al. (2006) has regarded the paired region of cVSC as vagal lobe, which shows TH-immunoreactivity in the Japanese eel. Mukuda and Ando (2003b) has referred to the postobecular region as CNC, where nerve fibers are distributed, but have not described origin of the fibers in the Japanese eel. In goldfish, on the other hand, these nuclei are clearly distinguished and their neurohistological features are well documented. The vagal lobe is hypertrophied dorsolaterally in the paired region and CNC is found in the commissural region exclusively (Morita and Finger 1987; Goehler and Finger 1992). CNC is known to receive viscerosensory inputs from the pharynx (Morita and Finger 1987; Goehler and Finger 1992) and is TH-immunopositive (Morita and Finger 1987). In addition, CNC has been reported to connect with vagal motoneurons in goldfish (Morita and Finger 1985; Goehler and Finger 1992). In the present study, we demonstrated that the vagal afferent from pharynx terminates in the paired region of cVSC which shows TH-immunoreactivity (Fig. 2b, d, e) and that cVSC controls the vagal motoneurons. In addition, TH-immunoreactive somata are localized within a rostrocaudally short range (ca. 84 μm) between the paired and commissural regions (Fig. 1f, Supplement figure 1c-i). In the eel, therefore, it may be reasonable that CNC is comparable to the region including the commissural and paired regions of cVSC but not postobecular region, and that vagal lobe corresponds to the rostral region of VSC as described in European eel (Roberts et al. 1989).

Some of BDA-10KF positive fibers end emerge as tubercles in cVSC in the

tracing study. Size of the tubercles is smaller (4-8 μm) than the cell body of TH-immunoreactive neuron (15-20 μm). In lamprey, electrosensory nerve forms extraordinarily large terminal (10-30 μm) as well as normal-sized terminal (1-3 μm) in the dorsal octavolateralis nucleus (Kishida et al. 1988; Koyama et al. 1993). Shape of the large terminal is circular or ellipsoidal (Koyama et al. 1993). The size and localization are different between the eel and lamprey but the shape of tubercle observed in the eel is similar to that of large terminal of the lamprey. Although fine analyses are needed, the tubercular structures seen in the eel VSC may be the terminals of vagal nerve from the pharynx.

Viscerotopic arrangement of the mGVC, noted in our previous study (Mukuda and Ando, 2003a), was confirmed in the present study. We were also able to determine the distribution of the motoneurons that innervate the pharyngeal wall or UES much finer scale than previously by using an improved method of the injection into UES in the present study. Longitudinally narrower distribution of the motoneurons of UES was found in the present study, compared previously. This may be caused by the diffusion of EB injected into the UES as well as unexpected variation of injection site within the UES. By inserting a mouthpiece into oral cavity to hold mouth opening widely and expose the UES, it became possible to inject the dye into a target point in the UES correctly in the present study. The method for injection into the UES is advantageous to discriminate the motoneurons which innervate the UES and those which innervate the other muscles adjacent to the UES since we observed in an individual animal that the mGVC motoneurons stained with BDA-10KF injected into the vagal nerve projecting to the pharyngeal wall and branchial arches are not labeled with EB injected into the UES (Fig. 2d-f).

A plausible function of the neuronal circuits on swallowing

In the Japanese eel, flow of ventilatory water across the gills is archived by combined actions of an increased intrapharyngeal pressure and UES closure. To generate ventilation cycle, rhythmic pharyngeal and continuous UES contractions are required. The rhythmic muscular contraction is generated by the rhythmic firing of the muscle motoneurons (Burleson and Smith 2001). While the contraction of UES, the motoneurons of UES would fire and release acetylcholine at the nerve endings continuously. The pharyngeal wall muscle and UES in the eel are striated, and are constricted by action of acetylcholine (Kozaka and Ando 2003). We demonstrated that the motoneurons of pharyngeal wall muscle and UES are located in the mGVC and are ChAT-immunoreactive. Compared with the results of retrograde tracing and electrophysiological experiments, distribution of the motoneurons of UES seems to be comparable to that of the continuously firing neurons within mGVC. On the other hand, restricted distribution of the rhythmically firing neurons is located in the mid region of mGVC where the motoneurons of pharyngeal wall and UES are co-existed.

Assuming that the neuronal activity recorded in the isolated brain represents that of an intact brain, we can conclude that the continuously firing motoneurons innervate the UES and the rhythmically firing motoneurons innervate the pharyngeal wall. The differing responsiveness of the rhythmically and continuously firing motoneurons to the cVSC stimulation forms the basis for explaining the regulation of the pharyngeal and UES reflexes during swallowing in the eel (Fig. 7). During swallowing, the cVSC is activated by vagal inputs from the pharynx, which are initiated

by physical stimuli, such as attachment of food or water to the pharyngeal wall. The stimulation of cVSC likely mimics neuronal inputs from the pharynx. To transport pharyngeal contents into the esophagus (i.e., facilitation of swallowing), cVSC relays signals to the motoneurons to constrict pharynx and to relax UES, simultaneously. Therefore, cVSC may coordinate the pharyngeal and upper esophageal muscular actions during swallowing.

The entrance to the esophagus is generally held closed by the contraction of UES in mammals. Hence, the relaxation of UES and contraction of pharynx is necessary to archive swallowing as in the eel. Mammalian UES is composed of several muscles including the cricopharyngeal muscle and action of the muscle is the most critical for proper functioning of UES. During the relaxation of UES, continuous firing of the cricopharyngeal muscle ceases transiently (Shipp et al. 1970; Asoh and Goyal 1978) and the break in firing may be induced by the inhibition of active motoneurons which innervate the cricopharyngeal muscle (Doty 1968; Zoungrana et al. 1997). The cricopharyngeal muscle is innervated by the nucleus ambiguus ipsilaterally (Bieger and Hopkins 1987; Kitamura et al. 1991; Kobler et al. 1994; Bao et al. 1995) and constricted by acetylcholine (Malmberg et al. 1991). Nucleus ambiguus receive the projections from nucleus of the solitary tract (Cunningham and Sawchenko 2000) which contains catecholaminergic neurons, i.e. A2 noradrenergic/C2 adrenergic neurons (Hollis et al. 2004). The cricopharyngeal muscle is commonly derived from the branchial arches and is composed of striated muscles in mammals and fish. The similarities in ontogeny, motoneuron innervation, and catecholamine sensitivity between the eel UES and mammalian cricopharyngeal muscle suggest that the mechanisms controlling UES action are similar among both fish and mammals. Thus our results may be useful for

understanding the origin of central regulation of the pharyngeal and UES reflexes in mammals.

In conclusion, the cVSC activates rhythmically firing neurons and inhibits continuously firing neurons in the eel mGVC. Inhibition is mediated, in part, by catecholamines. Our results demonstrate the functional significance of the connections between the viscerosensory and visceromotor neurons previously reported in teleosts. Based on this, we propose a model for the neuronal regulation on swallowing in fish, which may also be useful for understanding the origin of central regulation of the pharyngoesophageal stage of swallowing in mammals.

Acknowledgments

The present study was supported, in part, by Satake Foundation and by Grants-in-Aid for Scientific Research (C) no. 19570069 from the Ministry of Education, Culture, Sports, Science and Technology, Japan. Animal usage and all experimental procedures in the present study were approved by the Committee for Animal Experimentation of Hiroshima University and meet the guidelines of the Japanese Association for Laboratory Animal Science.

References

Anadón R, Molist P, Rodríguez-Moldes I, López JM, Quintela I, Cerviño MC, Barja P, González A (2000) Distribution of Choline acetyltransferase immunoreactivity in the brain of an elasmobranch, the lesser spotted dogfish (*Scyliorhinus canicula*). J Comp Neurol 420: 139-170

Arenzana FJ, Clemente D, Sánchez-González R, Porteros A, Aijón J, Arévalo R (2005) Development of the cholinergic system in the brain and retina of the zebrafish. Brain Res Bull 66: 421-425

Asoh R, Goyal RK (1978) Manometry and electromyography of the upper esophageal sphincter in the opossum. Gastroenterology 74: 514-520

Bao X, Wiedner EB, Altschuler SM (1995) Transsynaptic localization of pharyngeal premotor neurons in rat. Brain Res 696: 246-249

Barreiro-Iglesias A, Villar-Cerviño V, Villar-Cheda B, Anadón R, Rodicio MC (2008) Neurochemical characterization of sea lamprey taste buds and afferent gustatory fibers: presence of serotonin, calretinin, and CGRP immunoreactivity in taste bud bi-ciliated cells of the earliest vertebrates. J Comp Neurol 511: 438-453

Bieger D, Hopkins DA (1987) Viscerotopic representation of the upper alimentary tract in the medulla oblongata in the rat: the nucleus ambiguus. J Comp Neurol 262: 546-562

Broussard DL, Li H, Altschuler SM (1997) Colocalization of GABA (A) and NMDA receptors within the dorsal motor nucleus of the vagal nerve (DMV) of the rat. Brain Res 763: 123-126

Burleson ML, Smith RL (2001) Central nervous control of gill filament muscles in channel catfish. Respir Physiol 126: 103-112

Castro A, Becerra M, Anadón R, Manso MJ (2008) Distribution of calretinin during development of the olfactory system in the brown trout, *Salmo trutta fario*: Comparison with other immunohistochemical markers. J Chem Neuroanat 35: 306-316

Clemente D, Porteros A, Weruaga E, Alonso JR, Arenzana FJ, Aijón J, Arévalo R (2004) Cholinergic elements in the zebrafish central nervous system: Histochemical and immunohistochemical analysis. J Comp Neurol 474: 75-107

Cunningham ET Jr, Sawchenko PE (2000) Dorsal medullary pathways subserving oromotor reflexes in the rat: Implications for the central neural control of swallowing. J Comp Neurol 417: 448-466

Díaz-Regueira S, Anadón R (1992) Central projections of the vagus nerve in *Chelon labrosus* Risso (Teleostei, O. Perciformes). Brain Behav Evol 40: 297-310

Doty RW (1968) Neural organization of deglutition. In: Code CF (ed) Handbook of Physiology, Sect 6, Vol IV, American Physiological Society, Washington DC, pp 1861-1902

Feng HS, Lynn RB, Han J, Brooks FP (1990) Gastric effects of TRH analogue and bicuculline injected into dorsal motor vagal nucleus in cats. Am J Physiol 259: G321-326

Folgueira M, Anadón R, Yáñez J (2003) Experimental study of the connections of the gustatory system in the rainbow trout, *Oncorhynchus mykiss*. J Comp Neurol 465: 604-619

Fukuda A, Minami T, Nabekura J, Oomura Y (1987) The effects of noradrenaline on neurones in the rat dorsal motor nucleus of the vagus, in vitro. J Physiol 393: 213-231

Goehler LE, Finger TE (1992) Functional organization of vagal reflex systems in the

brain stem of the goldfish, *Carassius auratus*. J Comp Neurol 319: 463-478

Hayakawa T, Zheng JQ, Yajima Y (1997) Direct synaptic projections to esophageal motoneurons in the nucleus ambiguus from the nucleus of the solitary tract of the rat. J Comp Neurol 381: 18-30

Hollis JH, Lightman SL, Lowry CA (2004) Integration of systemic and visceral sensory information by medullary catecholaminergic systems during peripheral inflammation. Ann NY Acad Sci 1018: 71-75

Hudson LC (1986) The origins of innervation of the canine caudal pharyngeal muscles: an HRP study. Brain Res 374: 413-418

Ito S, Mukuda T, Ando M (2006) Catecholamines inhibit neuronal activity in the glossopharyngeal-vagal motor complex of the Japanese eel: significance for controlling swallowing water. J Exp Zool 305: 499-506

Kanwal JS, Caprio J (1987) Central projections of the glossopharyngeal and vagal nerves in the channel catfish, *Ictalurus punctatus*: clues to differential processing of visceral input. J Comp Neurol 264: 216-230

Kishida R, Koyama H, Goris RC (1988) Giant lateral-line afferent terminals in the electroreceptive dorsal nucleus of lampreys. Neurosci Res 6: 83-87

Kitamura S, Ogata K, Nishiguchi T, Nagase Y, Shigenaga Y (1991) Location of the motoneurons supplying the rabbit pharyngeal constrictor muscles and the peripheral course of their axons: a study using the retrograde HRP or fluorescent labeling technique. Anat Rec 229: 399-406

Kobler JB, Datta S, Goyal RK, Benecchi EJ (1994) Innervation of the larynx, pharynx, and upper esophageal sphincter of the rat. J Comp Neurol 349: 129-147

Koyama H, Kishida R, Goris R, Kusunoki T (1993) Giant terminals in the dorsal

octavolateralis nucleus of lampreys. J Comp Neurol 335: 245-251

Kozaka T, Ando M (2003) Cholinergic innervation to the upper esophageal sphincter muscle in the eel, with special reference to drinking behavior. J Comp Physiol [B] 173: 135-40

Laccasagne O, Kessler JP (2000) Cellular and subcellular distribution of the amino-3-hydroxy-5-methyl-4-isoxazole propionate receptor subunit GluR2 in the rat dorsal vagal complex. Neurosci 99: 557-563.

Ma PM (1994) Catecholaminergic systems in the zebrafish. I. Number, morphology, and histochemical characteristics of neurons in the locus coeruleus. J Comp Neurol 344: 242-255

Malmberg L, Ekberg O, Ekström J (1991) Effects of drugs and electrical field stimulation on isolated muscle strips from rabbit pharyngoesophageal segment. Disphagia 6: 203-208

Medda BK, Lang IM, Layman R, Hogan WJ, Dodds WJ, Shaker R (1994) Characterization and quantification of a pharyngo-UES contractile reflex in cats. Am J Physiol 267: G972-983

Morita Y, Finger TE (1985) Topographic and laminar organization of the vagal gustatory system in the goldfish, *Carassius auratus*. J Comp Neurol 238: 187-201

Morita Y, Finger TE (1987) Topographic representation of the sensory and motor roots of the vagus nerve in the medulla of goldfish, *Carassius auratus*. J Comp Neurol 264: 231-249

Mukuda T, Ando M (2003a) Medullary motor neurons associated with drinking behavior of Japanese eels. J Fish Biol 62: 1-12

Mukuda T, Ando M (2003b) Brain atlas of the Japanese eel: comparison to other fishes.

Memory of Faculty of Integrated Arts & Sciences, Hiroshima University Series IV 29: 1-25

Mukuda T, Matsunaga Y, Kawamoto K, Yamaguchi K, Ando M (2005) "Blood-contacting neurons" in the brain of the Japanese eel *Anguilla japonica*. J Exp Zool A 303: 366-376

Nabekura J, Ueno T, Katsurabayashi S, Furuta A, Akaike N, Okada M (2002) Reduced NR2A expression and prolonged decay of NMDA receptor-mediated synaptic current in rat vagal motoneurons following axotomy. J Physiol 539: 735-741

Pombal MA, Marín O, González A (2001) Distribution of choline acetyltransferase-immunoreactive structures in the lamprey brain. J Comp Neurol 431: 105-126

Pombal MA, Abalo XM, Rodicio MC, Anadón R, González A (2003) Choline acetyltransferase-immunoreactive neurons in the retina of adult and developing lampreys. Brain Res 993: 154-163

Roberts BL, Meredith GE, Maslam S (1989) Immunocytochemical analysis of the dopamine system in the brain and spinal cord of the European eel, *Anguilla anguilla*. Anat Embryol (Berl) 180: 401-412

Shipp T, Deatsch WW, Robertson K (1970) Pharyngoesophageal muscle activity during in man. Laryngoscope 80: 1-16

Sivarao DV, Krowicki ZK, Hornby PJ (1998) Role of $GABA_A$ receptors in rat hindbrain nuclei controlling gastric motor function. Neurogastroenterol Motil 10: 305-313

Sivarao DV, Krowicki ZK, Abrahams TP, Hornby PJ (1999) Vagally-regulated gastric motor activity: evidence for kainate and NMDA receptor mediation. Eur J Pharmacol 368: 173-182

Sueiro C, Carrera I, Rodríguez-Moldes I, Molist P, Anadón R (2003) Development of catecholaminergic systems in the spinal cord of the dogfish *Scyliorhinus canicula* (Elasmobranchs). Brain Res Dev Brain Res 142: 141-150

Travagli RA, Gillis RA, Rossiter CD, Vicini S (1991) Glutamate and GABA-mediated synaptic currents in neurons of the rat dorsal motor nucleus of the vagus. Am J Physiol 260: G531-536

Washabau RJ, Fudge M, Price WJ, Barone FC (1995) GABA receptors in the dorsal motor nucleus of the vagus influence feline lower esophageal sphincter and gastric function. Brain Res Bull 38: 587-594

Willis A, Mihalevich M, Neff RA, Mendelowitz D (1996) Three types of postsynaptic glutamatergic receptors are activated in DMNX neurons upon stimulation of NTS. Am J Physiol 271: R1614-1619

Zoungrana OR, Amri M, Car A, Roman C (1997) Intracellular activity of motoneurons of the rostral nucleus ambiguus during swallowing in sheep. J Neurophysiol 77: 909-922

Figure legends

Fig. 1. Motoneurons innervating the pharyngeal wall and upper esophageal sphincter (UES) within glossopharyngeal-vagal motor complex (GVC) and catecholaminergic neurons within the caudal region of viscerosensory column (cVSC) in the eel medulla. Representative transverse sections stained retrogradely with Evans blue (EB, *red*) injected into the pharyngeal wall (a) and UES (b). The sections were also immunostained with anti-choline acetyltransferase (ChAT, *blue*) and anti-tyrosine hydroxylase (TH, *green*) antibodies. Fluorescent image of EB alone (*left*) and a merged image of EB, ChAT, and TH (*right*). To intensify contrast, fluorescence of ChAT-immunoreactivity is expressed with blue color. (c) Low magnification view of the transverse section stained with anti-TH antibody (*green*) and EB (*red*) injected into the UES. Magnified view of the mid region of GVC (mGVC) (d) and cVSC (e) areas, enclosed by squares in (c). (f) Summary of distribution of the motoneurons stained with EB and TH-immunoreactive neurons rostrocaudally in the eel caudal medulla. The rostrocaudal level is expressed as the distance from the obex, the plus value meaning rostral to and the minus value caudal to the obex. Number of the eel examined in the analysis is indicated in parentheses. AP, area postrema; cGVC, caudal region of GVC; rGVC, rostral region of GVC; 4V, fourth ventricle.

Fig. 2. Sensory neurons projecting to the pharyngeal wall and branchial arches in the eel. (a) Schematic drawing of a transverse aspect in the eel caudal medulla (Mukuda and Ando 2003b). (b-d) Neurons traced by a biotinylated dextran amine conjugated with fluorescein isothiocyanate (BDA-10KF) injected into the vagal nerve projecting to the pharyngeal area. BDA-10KF-positive fibers were observed along the dorsal margin of

descending trigeminal root (DV) (n = 3) (at 56 μm rostral to the obex) (b), whereas their cell bodies were located in the nodose ganglion within the glossopharyngeal-vagal nerve (IX-X) (c). BDA-10KF-positive cell bodies in the nodose ganglion are denoted by 1, 2, and 3. Asterisk indicates a region containing a predominance of BDA-10KF positive fibers. Each region is shown by hatching in (a). (d) BDA-10KF-positive fibers with tubercles in cVSC (at 56 μm rostral to the obex) (n = 3). The inset shows a highly magnified view of the cVSC region enclosed by a square in the main diagram. The eel was injected concurrently with EB into the UES, and BDA-10KF into the vagal nerve projecting to the pharyngeal wall and branchial arches except for 3rd branchial arch. (e) Immunohistochemistry using anti-TH antibody in the section immediately rostral to (d) (at 70 μm rostral to the obex). Number in (d) and (e) is given for EB-positive neurons within mGVC. (f) Magnified view of the EB-positive neurons (*red*) numbered 4, 5, and 6 within the mGVC. Cven, commissura ventralis rhombencephali; MLF, medial longitudinal fascicle; RF, reticular formation; RInf, raphe nucleus inferior; SGT, secondary gustatory tract; TSV, vestibulo-spinal tract.

Fig. 3. Summary graph showing the number of recordings in the rostrocaudal position within mGVC. Rostrocaudal level is expressed as the distance from the obex, the plus value meaning rostral to and the minus value caudal to the obex.

Fig. 4. Extracellular recordings from the mGVC neurons. Spontaneous activity of mGVC neurons that fired: (a) at a multi-second burst interval (“rhythmically firing”) or (b) continuously (“continuously firing”). Solid circle in the rhythmically firing recording indicates the timing of spike appearance. (c) Single-unit discrimination of the

neuronal activity shown in (b). Four different single-units, denoted by a-d, were discriminated based on the width-amplitude plot (*left*) and frequency (*right*) during a 300 sec period of spontaneous activity.

Fig. 5. Effect of cVSC stimulation on the mGVC neurons. Activation of the rhythmically firing (a) and inhibition of the continuously firing (b) neurons in response to the cVSC stimulation. Arrow indicates the initiation of field stimulation in cVSC (0.5 mA, three trains of 0.1 msec pulse duration at 10 Hz). Timing of spike appearance in the trace of the rhythmically firing neurons is indicated by solid circle (before stimulation) and solid triangle (after stimulation). Open circle indicates the putative timing of spike appearance if stimulation is not applied. (c) Histogram showing the mean spike number in normal aCSF (Control, Wash out), in aCSF/1 μM prazosin (Prazosin), and in aCSF/1 μM yohimbine (Yohimbine) in each unit shown in (b). Mean spike number was calculated over five trials and was compared among a 5 sec period 30 sec before (pre), immediately after (stim), and 30 sec after (post) cVSC stimulation. Asterisk indicates significant differences (Tukey-Kramer test, $P < 0.01$). Row data in the presence of prazosin or yohimbine are shown on the right.

Fig. 6. Summary of the effect of the cVSC stimulation on the continuously firing mGVC neurons. Mean spike number during a 5 sec period either 30 sec before (pre, *circle*), immediately after (stim, *triangle*), or 30 sec after (post, *rectangle*) cVSC stimulation. Data is the mean of five trials for each unit. We compared the mean number of spikes between units, as in Fig. 5c.

Fig. 7. Summary diagram of the functional arrangement of mGVC neurons.

Supplement figure 1. Photomicrographs showing tyrosine hydroxylase (TH) immunoreactive neurons (*green*) in the caudal medulla in the Japanese eel (transverse section). The photomicrographs are arranged in the rostrocaudal order. To identify the area postrema (AP), which lacks the blood-brain barrier (BBB), the eels were injected with 200 μl of phosphate buffered saline (PBS, pH 7.4) containing sulfosuccinimidobiotin (50mg/ml, NHS, 21217, Pierce, Rockford, IL) (*red*) into the artery 30 min before transcardiac perfusion with saline and fixative. NHS binds to the blood proteins and forms a NHS-protein complex, and the complex would leak only at the brain region outside the BBB. TH-immunoreactive cell bodies are located inside the BBB in the paired and commissural regions rostrally (i.e. caudal region of viscerosensory column, cVSC) (a-i), whereas the neurons are located outside the BBB in the region caudal to the commissural region (i.e. AP) (j-p). Number denoted in each photomicrograph indicates rostrocaudal distance (in μm) from the obex, the plus value meaning rostral to and the minus value caudal to the obex.

Supplement figure 2. Photomicrographs showing the locations of recording and stimulation. (a) A horizontal section showing a recording site in the mid region of glossopharyngeal-vagal motor complex (mGVC), which was stained with Evans blue (EB) (*red*) injected into the upper esophageal sphincter (UES) 4 days before electrophysiology and immunostained with anti-ChAT (*blue*) and anti-TH (*green*) antibodies. The neuron positive both to EB and to anti-ChAT antibody simultaneously shows pink-colored. Arrowhead indicates the trace of tissue damage caused by the

insertion of recording electrode. Thick white broken line indicates the level of obex, which is a landmark structure terminating in the fourth ventricle (4V) caudally on the dorsal view of the brain. (b) A transverse section demonstrating the path of a recording electrode. The path of the insertion is shown with thin white broken line. The neurons stained by EB injected into UES are denoted by 1-4. (c) A transverse section showing the trace of attachment of stimulation electrode in cVSC. The path is marked with white broken line. Asterisk indicates midline. cGVC, caudal region of GVC.

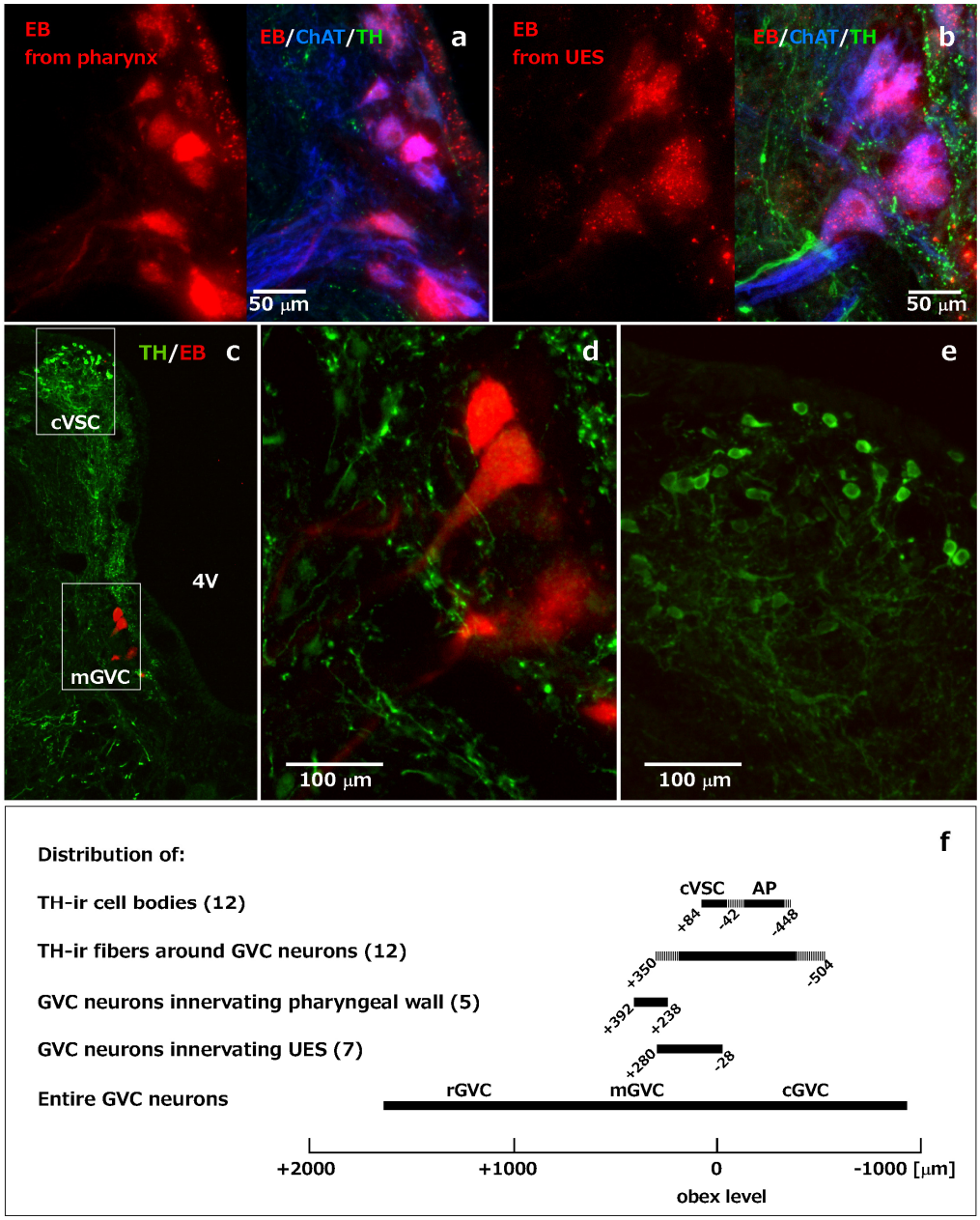

Fig. 1 Mukuda & Ando

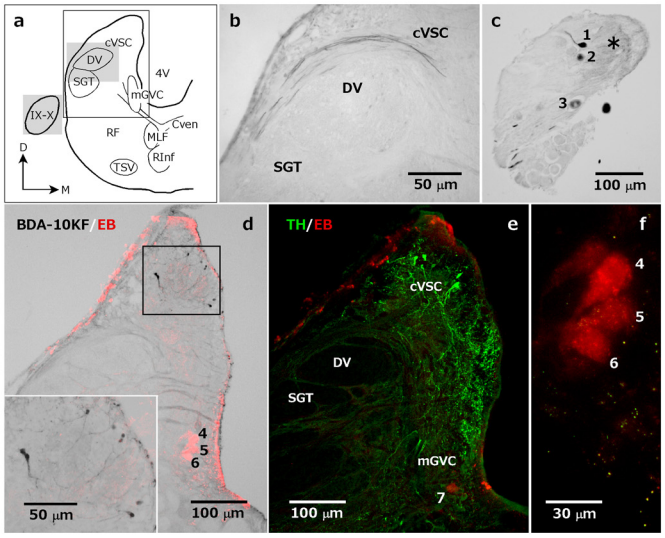

Fig. 2 Mukuda & Ando

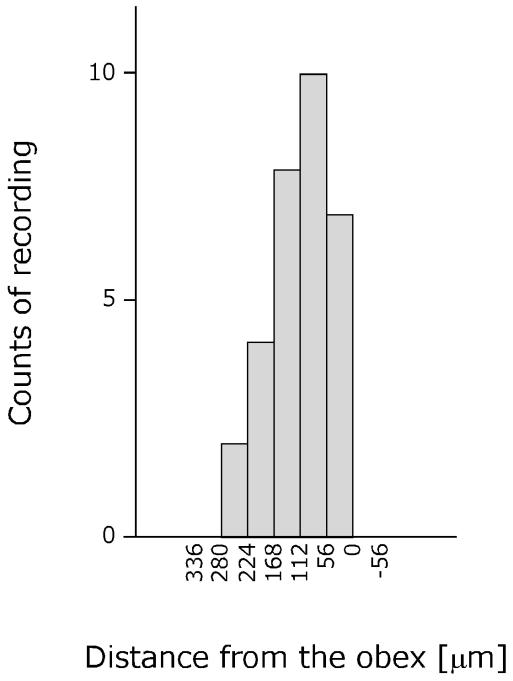

Fig. 3 Mukuda & Ando

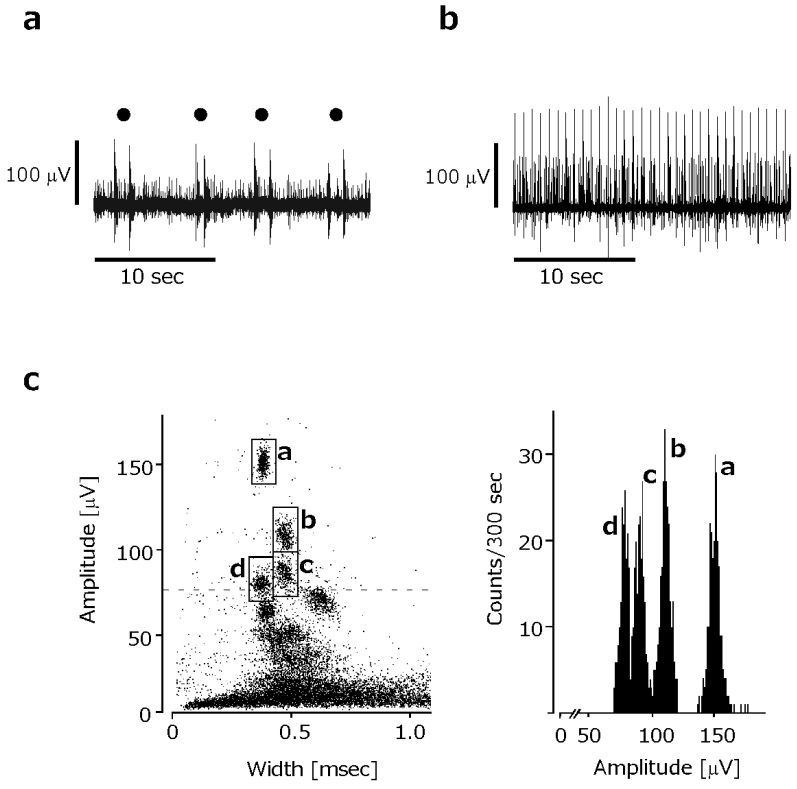

Fig. 4 Mukuda & Ando

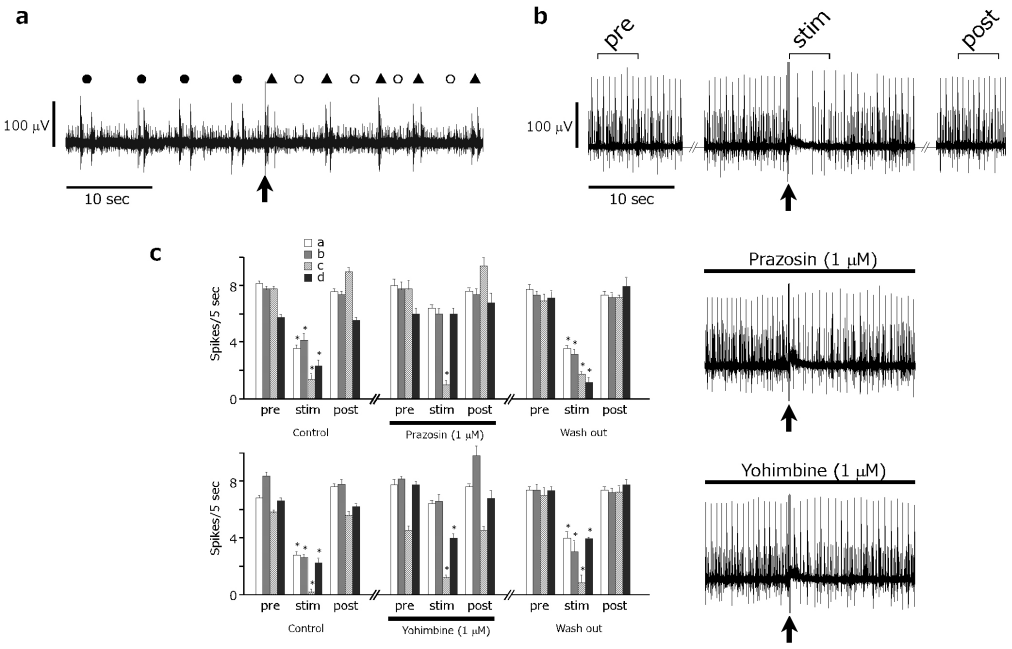

Fig. 5 Mukuda & Ando

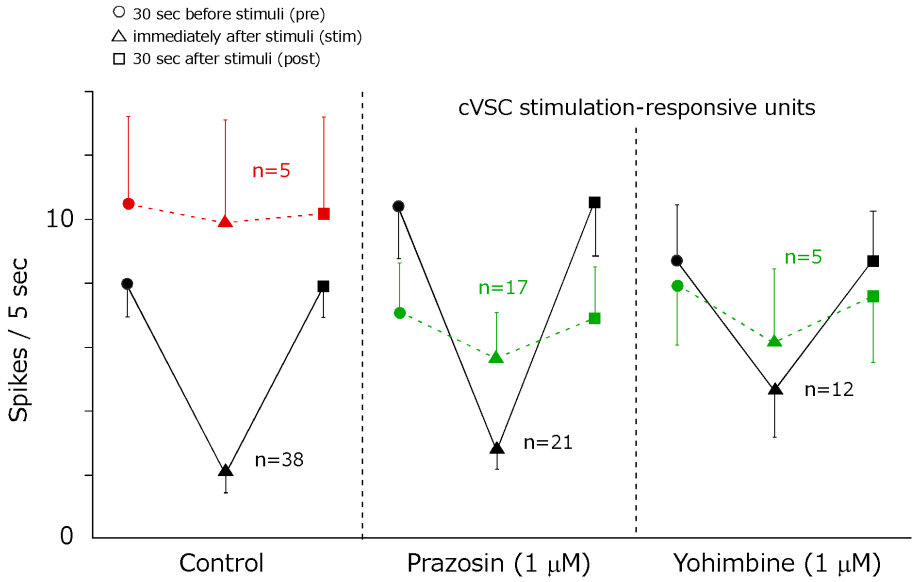

Fig. 6 Mukuda & Ando

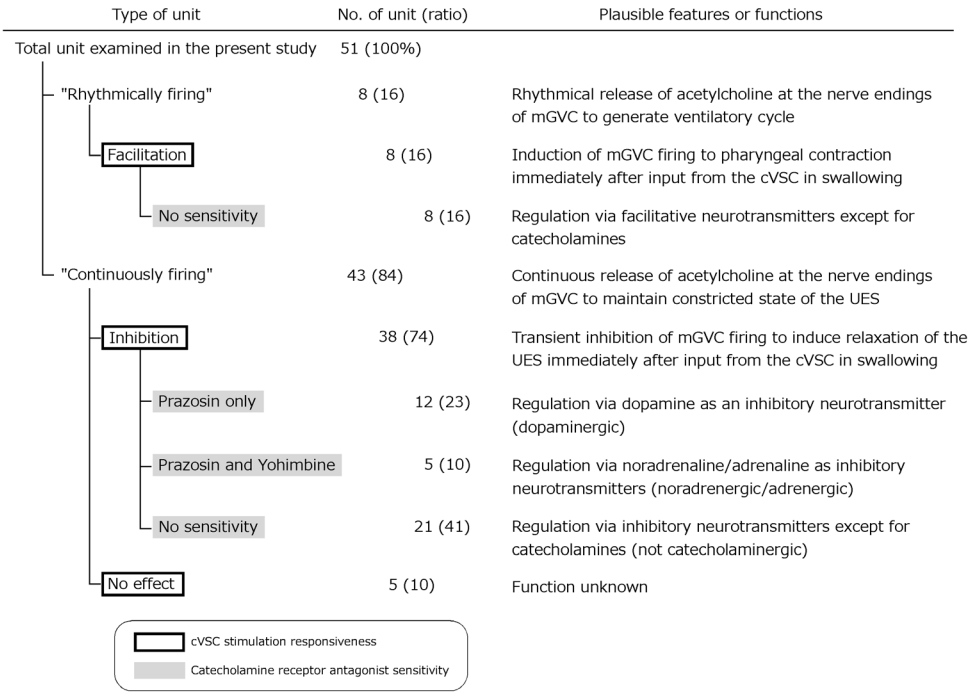

Fig. 7 Mukuda & Ando

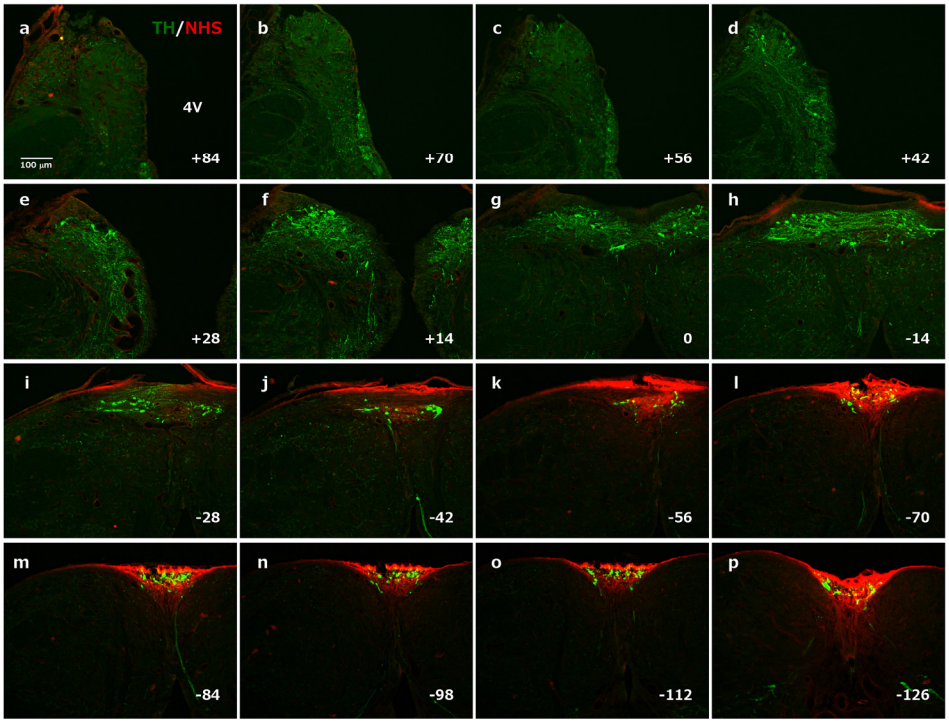

Supplement figure 1 Mukuda & Ando

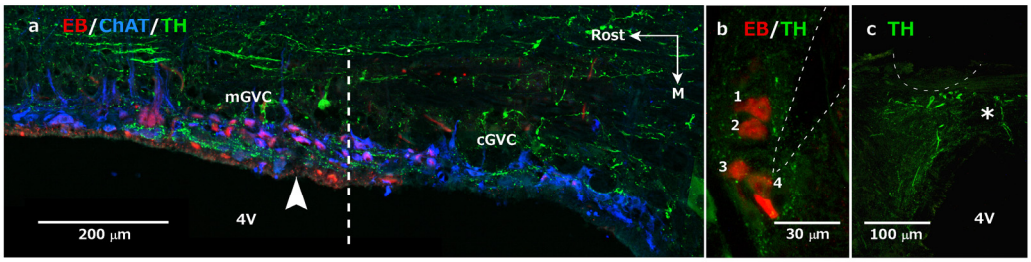

Supplement figure 2 Mukuda & Ando